Bax Channel Triplet: Cooperativity and Voltage Gating

Shang H. Lin, Nuval Cherian, Benjamin Wu, Hyo Phee, Christy Cho, Marco Colombini*

Department of Biology, University of Maryland, College Park, MD 20742

Tel: 301-405-6925 Fax: 301-314-9358
E-mail: colombini@umd.edu

* corresponding author

Keywords: mitochondria, planar membrane, Bcl-2, apoptosis, pore, dipole

Short (page heading) title: Bax Channel Triplet

Abbreviations: DPyPC, diphytanoylphosphatidylcholine;

Abstract

Bax, despite being a cytosolic protein, has the distinct ability to form channels in the mitochondrial outer membrane capable of releasing proteins that initiate the execution phase of apoptosis. When studied in a planar phospholipid membrane system full-length activated Bax can form conducting entities consistent with linearly organized three-channel units displaying steep voltage-gating (n=14) that rivals that of channels in excitable membranes. In addition the channels display strong positive cooperativity possibly arising from the charge distribution of the voltage sensors. Based on the functional behavior, one of the channels in this functional triplet is oriented in the opposite direction to the others often resulting in conflicts between the effects of the electric field and the positive cooperativity of adjacent channels. The closure of the first channel occurs at positive potentials and this permits the second to close but at negative potentials. The closure of the second channel in turn permits closure of the third but at positive potentials. Positive cooperativity manifests itself in a number of ways including the second and the third channels opening virtually simultaneously. This extraordinary behavior must have important although as yet undefined physiological roles.

Summary Statement

Bax forms voltage-gated channels with a steepness comparable to that of channels in excitable membranes. These channels are highly cooperative consistent with the fundamental conducting unit being a triplet of channels interacting through voltage-sensor dipoles.

Introduction

Voltage-gated membrane channels are proteins that have evolved to be especially sensitive to changes in membrane potential. They contain a voltage sensor whose movement is coupled to the conformational state of the protein which, in turn, determines the functional state of the channel: open or closed. Voltage-gated channels are mostly studied in cells that possess electrical excitability: muscles and neurons [1,2]. However, these are also found in other cell types (e.g. osteoblasts [3], endocrine cells [4], dynoflagellates [5], and bacteria [6]) and in intracellular membranes (e.g. tonoplasts [5], mitochondria [7]). Bax is a small (21.2 kDa) soluble cytosolic protein [8] that can be activated by pro-apoptotic signals, through an as yet unclear mechanism, to insert into the mitochondrial outer membrane to form membrane channels large enough to allow proteins to translocate [9–11]. Thus Bax is one of the killer proteins in the apoptotic process, initiating the execution phase of apoptosis. In addition, Bax can also form highly ordered, relatively small voltage-gated channels in phospholipid membranes [12]. Here we report that these channels show an unprecedented level of cooperativity and a steepness of voltage dependence that rivals that of the voltage-gated channels responsible for the electrical excitability of neurons and muscle cells.

Antonsson *et al.* [13] and Schlesinger *et al.* [14] were the first groups to study Bax channels on planar membranes using truncated Bax (BaxΔC19) and observed a variety of discrete changes in conductance interpreted as single channels. Rectification and changes in channel activity were observed when different voltages were applied. Later similar results were reported for full-length Bax [15]. Channels observed in mitochondria undergoing apoptosis (mitochondrial apoptosis-induced channel, MAC) were attributed to Bax [16]. In all these experiments, including those with MAC, no voltage gating was reported in the range of ±50 mV. Using improved techniques for handling Bax, we discovered that full-length Bax can form two types of channels (Type A and Type B), and one of them (Type A) is voltage-gated [12]. In 1.0 M KCl, Type A Bax channels have fundamental conductances of 1.5 ± 0.4 nS and 4.1 ± 0.7 nS, with the latter about 3 times of the former. Upon the application of high positive voltages on the side of Bax addition, Type A channels close in a series of uniform decrements (1.4 ± 0.3 nS). We now show that these have a preference for being organized into a triplet of channels with different functional properties.

The existence of double-barreled [17] and triple barreled channels [18] are well known but the triplets formed by Bax have an unprecedented combination of mixed orientation, cooperativity and very steep voltage gating. Indeed, different functionalities are observed depending on how the voltage is applied. A constant 70 mV potential results in closures of 3 individual channels in a manner similar to what was reported for a population of seemingly identical Type A channels (Fig. 1). However, the application of voltage ramps allowed us to discover striking differences between these channels of indistinguishable conductance. Each

channel has different voltage gating properties, responding to potentials of opposite sign, and together they show remarkable cooperativity. The cooperativity and voltage gating often conflict resulting is complex responses to time-dependent voltage changes. From these properties, we deduce a model of their structure and interaction consistent with all observations.

Experimental

Phospholipids were obtained from Avanti Polar Lipids (Alabaster, AL). Cholesterol was purchased from Sigma (St. Louis, MO).

Preparation of Bax

Recombinant full-length Bax was purified as previously published [8,12]. Only the soluble protein was recovered from the bacterial lysate leaving, any inclusion bodies behind. The soluble proteins was affinity purified by means of a self-cleavable intein tag. Glycerol was added (10% v/v) and then the solution shell-frozen in 100 µL aliquots in thin glass tubes using ethanol/dry ice and stored at < -80°C. Silver-staining following SDS-PAGE showed at least 95% monomeric Bax. The concentration of Bax was typically 15-35 µg protein/mL. Each aliquot was only thawed on ice right before an experiment.

Electrophysiological recordings

Planar phospholipid membranes were formed by the monolayer method [19,20]. The monolayers were formed by layering the lipid solution (0.5% (w/v) DPhPC, 0.5% (w/v) asolectin (polar extract of soybean phospholipids), and 0.05% (w/v) cholesterol in hexane) on the surface of the aqueous solutions (1.0 M KCl, 1 mM $MgCl_2$, and 5 mM PIPES, pH 6.9) on either side of the partition. The membrane was formed across a 0.1 mm hole in the partition. Calomel electrodes were used to interface with the aqueous phase. The membrane voltage was clamped using a high-quality operational amplifier in the inverted mode and the current recorded using Clampex 10.3 software. Data was generally low-pass filtered at 500 Hz but in some experiments this was reduced to 5 kHz. Typically 20-50µL of activated Bax was dispersed in 5mL aqueous solution on one side of the membrane. Bax was activated by exposing it to 1% (w/v) of β-octyl-glucoside for at least 30 minutes on ice [21,22]. No channel-forming activity was detected without this activation and addition of only the β-octyl-glucoside did not produce any channels.

All experiments reported were performed on Type A Bax channels. More than half of the experiments performed yielded Type A channels, the rest were Type B. Type A channels are voltage-gated and display a low level of current fluctuation, other than gating. Type B channels are not voltage-gated and have a much higher level of current noise. Voltage ramps were applied to investigate the behavior of these channels and determine their voltage-gating parameters. All the results reported were observed in at least 3 independent experiments, with usually multiple repeats of the illustrated behavior within each experiment.

Quantification of voltage dependence

The Boltzmann distribution was used to determine the parameters of voltage dependence. $\frac{P_O}{P_C} = e^{-\frac{\Delta E}{RT}}$.

$$\Delta E = nFV_0 - nFV = nF(V - V_0)$$

$$\ln(\frac{G_{max} - G}{G - G_{min}}) = \frac{nF}{RT}(V - V_0),$$

where P_O and P_C are the probability of the channels being in the open and closed state, respectively. ΔE is the energy difference between open and closed state. nFV_0 is the energy difference in the absence of a membrane potential, whereas nFV is the voltage-dependent energy difference. n is the number of charges that would need to move across the entire electric field to account for the voltage dependence, and V_0 is the voltage at which half of the channels on the membrane are open. G, G_{max}, and G_{min} are the conductance at any voltage, the maximal conductance and the minimal conductance, respectively (Fig. S1 in the Supplemental Data). Important conditions for using the Boltzmann distribution are: (1) the channel only has two states, open and closed; (2) the distribution is determined at equilibrium. When using voltage ramps, the rate of change in voltage may be too fast to allow the system to reach equilibrium. Therefore, we determined the value of "n" at various rates of voltage change and extrapolated the fitted line of the n vs. rate plot to zero rate in order to estimate the value of 'n' at equilibrium. For single-triplet experiments, we averaged the current records from at least 20 consecutive triangular ramps and for multi-triplet experiments, we averaged the records from at least 5 ramps to obtain valid parameters. The use of voltage steps to collect data for conductance voltage curves is problematic for large channels because keeping the channel at a fixed voltage for some time results in time-dependent adaptation to the voltage which differs from one voltage level to the next, degrading the information that is obtained.

Statistical analysis

Aggregate results are reported as an average ± one standard deviation with the number of independent experiments indicated in parentheses. The symbol, N, is used to indicate the number of experiments performed with a specific protocol. Unless otherwise specified, the probability to observe the behaviors reported here when we tested the protocols is 100%. Significant differences in values were tested using the Student's t-test.

Results

The dispersal of activated full-length Bax protein (21.2 kDa) in the aqueous phase next to a phospholipid membrane results in increases in permeability, characteristic of the formation of membrane channels. Of the two types of channels that form [12], one (Type A), is highly ordered (30 experiments, 59% of all experiments). As expected for channels, the permeability formed is a multiple of a fundamental unit, 4.5 nS (Fig. 1). What is unusual is that this unit has properties consistent with a triplet of channels (designated channel ①, ② and ③) that are highly cooperative and voltage gated (70 mV was applied after the break in Fig. 1). Each channel in the triplet is likely an oligomer of Bax. The formation of the permeability occurs rapidly even for a multiunit event (Fig. S2). The 110 nS permeability formed within 2 ms. As previously reported, the application of a constant voltage results in stepwise conductance decrements (Fig. S3) consistent with the closure of individual channels and the simplest explanation would be that a population of identical channels inserted together perhaps as a preformed aggregate or crystal. However, further analysis reveals complex properties. The application of 7.38 mV/sec voltage ramps to a single conductance unit (4.4 nS in this case) shows the total absence of voltage gating for several cycles. Remarkably, following a single conductance drop of 1.5 nS, gating was evident in ALL 90 subsequent ramp cycles performed in that experiment (Fig. 2 only shows the first 4). The first conductance drop (channel ①) occurred at a high positive potential (98 mV for the example shown in Fig. 2, 86 ± 14 (5) mV), consistent with experiments in which a constant voltage was applied. The subsequent gating (channel ②) took place at negative voltages (V_0 = -27 ± 4 (4) mV for 7.38 mV/sec ramps) with reopening taking place as the potential became more positive. Thus the gating took place between 2.9 and 1.5 nS consistent with gating of only channel ②**.** The average values of these intermediate conductance levels from 5 experiments are: 2.93 ± 0.06 and 1.45 ± 0.13 nS (Fig. S5). The closure of channel ② not only occurred at each subsequent cycle but it occurred within a very narrow voltage range, indicating a high steepness of voltage dependence (Fig. 3). This pattern of gating was highly reproducible and was evident both in membranes with a single 4.5 nS unit conductance and those with many units (Fig. S6). Within each of the 5 single-triplet experiments, the chance of observing a closure of channel ②, among all the ramps, was 92 ± 5 (5)% (total of 215 ramps at slow rates between 4.3 to 7.4 mV/sec). The closing of channel ③ took place only rarely with a slow voltage ramps but occurred more often at *higher* rates of change in voltage (Fig. S7, S8, 3). For example, the occurrence of the closure of channel ③ changes from 26 ± 18 % (in 215 ramps) to 84 ± 6 % (in 67 ramps) when the rate of voltage change was increased. Channel ③ closure occurred at positive potentials with the V_0 of 28 ± 2 (4) mV and reopening occurred as the positive potential declined (Fig. S9).

These results and others presented below can be understood in the context of the model illustrated in Fig. 4 (Fig. S4 for colored version). Although this is merely a model, its success in explaining rather complex behavior gives it some degree of solidity. Alternatives that we can conceive are far more complex and thus far less attractive. We propose that the fundamental conducting unit of 4.5 nS is a triplet of structurally identical channels in a linear organization (Fig. 4). A linear organization seems to best represent the functional behavior, since channel ① only affects the gating of channel ②, and closure/reopening of channel ③ is tightly related to the state of channel ②. From the sign of the voltage at which the channels gate, it is proposed that channel ① & ③ are oriented in one direction and ② is oriented in the opposite direction (shading direction indicates orientation). The arrows in the individual channels describe the orientation of the voltage sensor as a dipolar charge asymmetry and this direction inverts upon voltage-dependent channel closure. Note that this is NOT the orientation of the channel itself, just the voltage sensor domain. The orientation of the voltage sensor illustrated accounts for the sign of the voltage gating as observed experimentally (Fig. 3). Each channel is most likely an oligomer of Bax proteins [23] and the uniformity of the conductance decrements following the application of a constant 70 mV potential [12] argues strongly for structurally identical channels, each with the same number and organization of monomers. The behavior described is best explained by a strong positive cooperativity between the channels at the site of channel-channel interaction. The cooperativity strongly favors the channels to be in the same conformational state, either all open or all closed. The dipolar charge asymmetry of the voltage sensor could contribute or perhaps be THE CAUSE of the strong cooperativity. Thus closure of the first channel is unfavored (i.e. slow rate of closure even at high positive potentials probably due to the positive cooperativity between ① and ②). When it occurs it requires a high positive potential (Fig. 3) and is due to the closure of either channel ① or ③. As these are identical in location and interaction, once one of these closes, that one is defined as channel ①. Closure of channel ① not only removes the inhibition of closure on channel ② (the dipole-dipole interaction) but actually favors the closure of ②. Thus only a smaller potential is needed to close channel ② and the kinetics of this process are fast (i.e., gating of channel ② by triangular voltage ramps takes place with remarkable regularity, Fig. 2 and rabbit symbol in Fig. 4). For channel ③ to close, it requires both a positive potential and a closed ② (the positive potential acting on the voltage sensor dipole and closure of channel ② removing the favorable dipole-dipole interaction). However, a positive potential also leads to channel ② reopening and thus ③ does not have the conditions for closure. By using a higher rate of voltage change one takes advantage of the relatively slow reopening kinetics of channel ② and thus achieve the conditions necessary for the closure of channel. Fig. S7 shows the two outcomes of rising voltages from negative to positive values, either channel

② reopens or channel ③ closes. At elevated positive potentials both must be open or both closed. From what we observed, the reopening of channel ② and ③ is highly dependent on the rate of voltage change, meaning that the reopening process is slow and thus kinetically delayed. The closing process is much faster and thus it was the closing process that was analyzed to determine the voltage-dependent parameters (Fig. 5). Note that the mid-point of the voltage range at which the gating occurred, $V_{0,}$ of the closure process and that of the reopening process became the same as the rate of voltage change tended toward zero.

The slow kinetics of reopening is evident from the shift in the voltage at which channel ② reopens (Fig. S5, 5). At the higher rate of voltage change, the reopening of channel ② is delayed allowing one to achieve conditions suitable for ③ closure (Fig. S9). Once channel ③ closes, ② is inhibited from reopening due to the effects of cooperativity (Fig. 3) (note the favorable dipole-dipole interaction, Fig. 4). Indeed, when channel ③ is closed, the reopening of ② occurs virtually simultaneously with the reopening of channel ③ (Fig. 6), demonstrating strong cooperativity. Indeed the two re-openings occurred simultaneously at the degree of temporal resolution used in the experiments: 2 to 5 msec depending on the experiment.

The model also explains the staircase of closing events when a constant 70 mV potential is applied (Fig. S3). At constant high positive potential, the closure of channels ① and ③ is favored. When both of these are closed, the strong cooperative effect allows channel ② to close despite the wrong sign of the potential (Fig. 1). The conflicting actions of the electric field and the cooperativity result in a slow rate of closure indicated by the snail in Fig. 4.

Further evidence of the model comes from its ability to account for conductance changes observed with multi-unit experiments. In Fig. 7*A*, only 4 closures of channel ② were observed. This indicates that 4 channel ①'s (1.5 × 4 = 6 nS) must have been closed beforehand to allow these channel ②'s to close. Therefore, the all-open conductance should be 21 + 6 = 27 nS, equivalent of 6 conducting units. The remaining conductance after the 4 channel ② closures is consistent with 4 open channel ③'s (4 × 1.5 nS) plus 2 triplets (2 × 4.5 nS) that were not gating resulting in as total conductance of 15 nS. This interpretation is further illustrated in an experiment with many triplet units (Fig. 7*B*). Following the same logic, the total conductance on the left panel is consistent with about 19 non-gating triplets (all channels open) and 11 gating triplets (determined from channel ② closures). A 70 mV potential was applied for 82 s resulting in the equivalent of *16*, 1.5 nS conductance decrements, presumably from more channel ①'s being closed. The reapplication of a triangular voltage ramp resulted in 38 nS worth of channel ② gating, consistent with *14* more gating triplets. Again the model explains the observed conductance changes. Finally, we used a voltage pulse sequence that allowed rapid closure of channel ② and ③ by applying a negative potential followed by a positive potential (Fig. S10). In

illustrated experiment, a negative potential caused immediate closure of two channel ②'s followed by a step to a positive potential resulting in immediate closure of two channel ③'s. Paired reopening of ② & ③ in two double-channel steps resulted in return to the initial conductance.

The rapid kinetics of channel ② closure allowed us to assume the achievement of a quasi-equilibrium between the open and closed state during the voltage change resulting from the applied triangular voltage ramp. Therefore a measure of the effective gating charge, n, was obtained by fitting to the Boltzmann distribution (Fig. S1). These values depended on the rate of change in voltage indicating that the kinetics of the process was still limiting. Thus the values of n were plotted against the rate of voltage change and its value at zero rate was determined by extrapolation. The resulting n of 14 ± 2 rivals those of the voltage-gated channels responsible for the electrical excitability of neurons and muscles (Fig. 8).

Discussion

The electrophysiological properties of Bax channels strongly support the conclusion that these are organized in a triplet structure in which the channels exhibit a high degree of positive cooperativity and steep voltage dependence. The channels prefer to be in the same state whether it be the closed or open state. Further, this cooperativity seems to be limited to pairs of likely adjacent channels: ①/② and ②/③. The voltage-dependent closure of channel ① & ③ at positive potentials and channel ② at negative potentials is most simply explained by channel ② being oriented in an opposite direction to ① & ③. This opposite orientation could account for the cooperativity if it were based on a charge dipole of the voltage sensor. An opposite orientation of adjacent channels would result in a favorable dipole-dipole interaction (①/② and ②/③) (Fig. 4). The movement across the membrane of the voltage sensor upon channel closure would invert the dipole (invert the direction of arrows in Fig. 4) resulting in electrostatic repulsion rather than attraction between adjacent channels and thus favor closure of the adjacent one. This model works best if the triplet is organized as a linear arrangement of channels, with channel ② in between ① & ③. Thus channel ① and ③ are essentially identical but their behavior differs once one of these closes. The steepness of the voltage dependence and thus the requisite movement of a large amount of gating charge from one side of the membrane to the other in opposite directions cannot be easily explained by anything other than an opposite orientation for these channels, despite the obvious concerns on how that could take place. Typically the channel's structure, such as a large surface domain (e.g. α- hemolysin [24]), limits insertion in only one direction. However VDAC channels have been shown to be able to insert into planar membranes in both directions [25,26]. In addition, colicins, toxin channels that have been reported to have similarities to Bcl-2 family proteins, translocate most of their mass to the opposite membrane surface when they insert into a phospholipid membrane [27]. Thus there is no serious theoretical impediment to the possibility of Bax channels inserting in opposite directions save those arising from the need to be skeptical with regard to any novel proposal.

A Boltzmann distribution analysis of the voltage dependent conductance of channel ② yielded an estimate of the effective gating charge. The value of 14 that was obtained is twice that reported for the voltage gated channels responsible for electrical excitability in animal cells when channel activation was analyzed by similar methods [1,28]. When charge was estimated by measuring displacement currents [28,29] then values comparable to those reported here were obtained. Thus the steepness of voltage gating we observed is extremely high indicating an as yet undefined but important role in the physiological function of Bax. The closure instead of the reopening process was used for analyzing both channel ② and ③ gating here, due to the substantial kinetic delay of the reopening process (Fig. 5). The delay makes one unable to study the gating of the channel with the assumption that it's very close

to equilibrium. Therefore, the one with less delay, the closure, was used here. The calculated parameters that define the gating process, n and V_0, should be the same regardless of which process is analyzed, the reopening or the closing process. However, we found that, although the V_0 of closure and reopening extrapolate to the same value at zero rate of voltage change, the n values don't seem to do this (Fig. S11). It may due to our inability to measure these values at low enough rates combined with a non-linear rate dependence of this value. It is also possible that the gating process exhibits true hysteresis. An explanation may emerge as more information about the gating mechanism is uncovered.

The very steep voltage dependence requires a highly charged voltage sensor domain and that can be reconciled with the protein structure if each channel is an oligomer of numerous Bax proteins. The oligomeric nature of the Bax channel is well accepted in the literature and there are various insights into how this oligomerization might take place [11,30–33]. Furthermore, studies have provided compelling evidence that helices 5, 6 and 9 are inserted into the membrane [34,35]. The high positive charge of helix 5 makes this helix an attractive candidate for the voltage sensor. Positively charged helices have been shown to be the voltage sensors in the $Na^+/K^+/Ca^{2+}$ family of voltage-gated channels [36].

The structure of Bax in the mitochondrial outer membrane and the properties of Bax channels have been studied extensively, but the overall level of understanding is quite limited. For example, the number of monomers per functional channel is still not clear. This number varies from four [37] to greater than a hundred [38]. Similar studies of the MAC channel [16] are consistent with channels of varying size. The published properties of conductances formed by the Bax protein also vary in magnitude. Some of this variation may arise from a heterogeneity of channel sizes and some from the source or treatment of the protein. Certainly the Type B channels formed by Bax vary in size probably because they can grow to any size. None of the published conductances clearly correspond to the properties of the Type A channels reported here. The reasons for these differences may have to do with methods of protein isolation and handling. Also the MAC channel being obtained from mitochondria undergoing apoptosis, is likely to be a far more complex structure that one formed from pure Bax protein.

The physiologically relevant role of the characteristics presented here is not clear yet. Obviously voltage gating of Bax channels requires a controllable potential across the mitochondrial outer membrane (MOM). Although somewhat controversial, the potential across the MOM was measured to be about -30-40 mV [39,40], and calculated to be able to reach a magnitude of ~60 mV [41]. The potential would be very sensitive to the dynamic flux of charged metabolites [41] and the charge of macromolecules in the cytosol and intermembrane space [39]. These change during the apoptotic process and thus could influence the conformational state of Bax channels. Another voltage gated channel exists in

the MOM: the VDAC channel. VDAC is found in all eukaryotic kingdoms and responsible for metabolite flux across the MOM. The canonical isoform has remarkably conserved voltage gating parameters [42,43] indicating strong evolutionary selection. Yet, voltage gating can easily be altered by single point mutations without affecting channel formation or metabolite flux [44]. Thus, the voltage-gating properties are conserved to allow VDAC to be controlled by the potential across the MOM. Similarly, the properties of Bax may have evolved to respond to the same potential.

Acknowledgements

We thank Richard Youle for providing us with the plasmid of full-length Bax, and Rachel Peissner and Toan Nguyen for helping with the experiments on planar membranes.

Funding

This work was funded by NSF [MCB-1023008].

Author contribution

Shang H. Lin, Nuval Cherian, Benjamin Wu, Hyo Phee, Christy Cho, Marco Colombini designed the research, performed the research, and analyzed the data. Shang H. Lin and Marco Colombini wrote the paper.

References

1 Hodgkin, A. L. and Huxley, A. F. (1952) A quantitative description of membrane current and its application to conduction and excitation in nerve. J. Physiol. **117**, 500–544.

2 Hille, B. (2001) Ion Channels of Excitable Membranes 3rd ed., Sinauer Associates, Inc.

3 Kizer, N., Harter, L., Hruska, K., Alvarez, U. and Duncan, R. (1999) Volume regulatory decrease in UMR-106.01 cells is mediated by specific alpha1 subunits of L-type calcium channels. Cell Biochem. Biophys. **31**, 65–79.

4 Best, L., Brown, P. D., Sener, A. and Malaisse, W. J. (2010) Electrical activity in pancreatic islet cells: The VRAC hypothesis. Islets **2**, 59–64.

5 DeCoursey, T. E. (2013) Voltage-gated proton channels: molecular biology, physiology, and pathophysiology of the H(V) family. Physiol. Rev. **93**, 599–652.

6 Bainbridge, G., Gokce, I. and Lakey, J. H. (1998) Voltage gating is a fundamental feature of porin and toxin beta-barrel membrane channels. FEBS Lett. **431**, 305–308.

7 Colombini, M. (2012) Mitochondrial Outer Membrane Channels. Chem. Rev. **112**, 6373–6387.

8 Suzuki, M., Youle, R. J. and Tjandra, N. (2000) Structure of Bax: coregulation of dimer formation and intracellular localization. Cell **103**, 645–654.

9 Kuwana, T., Mackey, M. R., Perkins, G., Ellisman, M. H., Latterich, M., Schneiter, R., Green, D. R. and Newmeyer, D. D. (2002) Bid, Bax, and lipids cooperate to form supramolecular openings in the outer mitochondrial membrane. Cell **111**, 331–342.

10 Kim, H., Rafiuddin-Shah, M., Tu, H.-C., Jeffers, J. R., Zambetti, G. P., Hsieh, J. J.-D. and Cheng, E. H.-Y. (2006) Hierarchical regulation of mitochondrion-dependent apoptosis by BCL-2 subfamilies. Nat. Cell. Biol. **8**, 1348–1358.

11 Bleicken, S., Classen, M., Padmavathi, P. V. L., Ishikawa, T., Zeth, K., Steinhoff, H.-J. and Bordignon, E. (2010) Molecular details of Bax activation, oligomerization, and membrane insertion. J. Biol. Chem. **285**, 6636–6647.

12 Lin, S. H., Perera, M. N., Nguyen, T., Datskovskiy, D., Miles, M. and Colombini, M. (2011) Bax forms two types of channels, one of which is voltage-gated. Biophys. J. **101**, 2163–2169.

13 Antonsson, B., Conti, F., Ciavatta, A., Montessuit, S., Lewis, S., Martinou, I., Bernasconi, L., Bernard, A., Mermod, J., Mazzei, G., Maundrell, K., Gambale, F., Sadoul, R., and Martinou, J-C. (1997) Inhibition of Bax Channel-Forming Activity by Bcl-2. Science **277**, 370–372.

14 Schlesinger, P. H., Gross, A., Yin, X. M., Yamamoto, K., Saito, M., Waksman, G. and Korsmeyer, S. J. (1997) Comparison of the ion channel characteristics of proapoptotic BAX and antiapoptotic BCL-2. Proc. Natl. Acad. Sci. U.S.A. **94**, 11357–11362.

15 Rostovtseva, T. K., Antonsson, B., Suzuki, M., Youle, R. J., Colombini, M. and Bezrukov, S. M. (2004) Bid, but not Bax, regulates VDAC channels. J. Biol. Chem. **279**, 13575–13583.

16 Martinez-Caballero, S., Dejean, L. M., Kinnally, M. S., Oh, K. J., Mannella, C. A. and Kinnally, K. W. (2009) Assembly of the mitochondrial apoptosis-induced channel, MAC. J Biol Chem. **284**, 12235–12245.

17 Miller, C. and White, M. M. (1984) Dimeric structure of single chloride channels from Torpedo electroplax. Proc. Natl. Acad. Sci. U.S.A. **81**, 2772–2775.

18 Weiss, M. S., Wacker, T., Weckesser, J., Welte, W. and Schulz, G. E. (1990) The three-dimensional structure of porin from Rhodobacter capsulatus at 3 A resolution. FEBS Lett. **267**, 268–272.

19 Montal, M. and Mueller, P. (1972) Formation of bimolecular membranes from lipid monolayers and a study of their electrical properties. Proc. Natl. Acad. Sci. U.S.A. **69**, 3561–3566.

20 Colombini, M. (1987) Characterization of Channels Isolated from Plant Mitochondria. Method Enzymol. **148**, 465.

21 Hsu, Y. T. and Youle, R. J. (1997) Nonionic detergents induce dimerization among members of the Bcl-2 family. J. Biol. Chem. **272**, 13829–13834.

22 Gross, a, Jockel, J., Wei, M. C. and Korsmeyer, S. J. (1998) Enforced dimerization of BAX results in its translocation, mitochondrial dysfunction and apoptosis. EMBO J. **17**, 3878–3885.

23 Eskes, R., Desagher, S., Antonsson, B. and Martinou, J. C. (2000) Bid induces the oligomerization and insertion of Bax into the outer mitochondrial membrane. Mol. Cell. Biol. **20**, 929–935.

24 Henrickson, S. E., DiMarzio, E. A., Wang, Q., Stanford, V. M. and Kasianowicz, J. J. (2010) Probing single nanometer-scale pores with polymeric molecular rulers. J. Chem. Phys. **132**, 135101-135108.

25 Zizi, M., Thomas, L., Blachly-Dyson, E., Forte, M. and Colombini, M. (1995) Oriented Channel Insertion Reveals the Motion of a Transmembrane Beta Strand During Voltage Gating of VDAC. J. Membr. Biol. **144**, 121–129.

26 Xu, X. and Colombini, M. (1996) Self-catalyzed insertion of proteins into phospholipid membranes. J. Biol. Chem. **271**, 23675–23682.

27 Kienker, P. K., Jakes, K. S. and Finkelstein, A. (2000) Protein translocation across planar bilayers by the colicin Ia channel-forming domain: where will it end? J. Gen. Physiol. **116**, 587–598.

28 Schoppa, N. E., McCormack, K., Tanouye, M. A., and Sigworth, F. J. (1992) The size of gating charge in wild-type and mutant Shaker potassium channels. Science **255**, 1712–1715.

29 Aggarwal, S. K. and MacKinnon, R. (1996) Contribution of the S4 segment to gating charge in the Shaker K+ channel. Neuron **16**, 1169–1177.

30 Dewson, G., Ma, S., Frederick, P., Hockings, C., Tan, I., Kratina, T. and Kluck, R. M. (2012) Bax dimerizes via a symmetric BH3:groove interface during apoptosis. Cell Death Differ. **19**, 661–670.

31 Czabotar, P. E., Westphal, D., Dewson, G., Ma, S., Hockings, C., Fairlie, W. D., Lee, E. F., Yao, S., Robin, A. Y., Smith, B. J., Huang, D. C. S., Kluck, R. M., Adams, J. M., and Colman, P. M. (2013) Bax crystal structures reveal how BH3 domains activate Bax and nucleate its oligomerization to induce apoptosis. Cell **152**, 519–531.

32 Zhang, Z., Zhu, W., Lapolla, S. M., Miao, Y., Shao, Y., Falcone, M., Boreham, D., McFarlane, N., Ding, J., Johnson, A. E., Zhang, X. C., Andrews, D. W., and Lin, J. (2010) Bax forms an oligomer via separate, yet interdependent, surfaces. J. Biol. Chem. **285**, 17614–17627.

33 George, N. M., Evans, J. J. D. and Luo, X. (2007) A three-helix homo-oligomerization domain containing BH3 and BH1 is responsible for the apoptotic activity of Bax. Genes Dev. **21**, 1937–1948.

34 García-Sáez, A. J., Mingarro, I., Pérez-Payá, E. and Salgado, J. (2004) Membrane-insertion fragments of Bcl-xL, Bax, and Bid. Biochemistry **43**, 10930–10943.

35 Annis, M. G., Soucie, E. L., Dlugosz, P. J., Cruz-Aguado, J. A., Penn, L. Z., Leber, B. and Andrews, D. W. (2005) Bax forms multispanning monomers that oligomerize to permeabilize membranes during apoptosis. EMBO J. **24**, 2096–2103.

36 Noda, M., Shimizu, S., Tanabe, T., Takai, T., Kayano, T., Ikeda, T., Takahashi, H., Nakayama, H., Kanaoka, Y. and Minamino, N. (1984) Primary structure of Electrophorus electricus sodium channel deduced from cDNA sequence. Nature **312**, 121–127.

37 Saito, M., Korsmeyer, S. J., Schlesinger, P. H., Farber, D. and Hughes, H. (2000) Bax-dependent transport of cytochrome c reconstituted in pure liposomes. Nat. Cell Biol. **2**, 553–555.

38 Nechushtan, A., Smith, C. L., Lamensdorf, I., Yoon, S. H. and Youle, R. J. (2001) Bax and Bak coalesce into novel mitochondria-associated clusters during apoptosis. J. Cell Biol. **153**, 1265–1276.

39 Colombini, M. (2004) VDAC: the channel at the interface between mitochondria and the cytosol. Mol. Cell Biochem. **256-257**, 107–115.

40 Porcelli, A. M., Ghelli, A., Zanna, C., Pinton, P., Rizzuto, R. and Rugolo, M. (2005) pH difference across the outer mitochondrial membrane measured with a green fluorescent protein mutant. Biochem. Biophys. Res. Commun. **326**, 799–804.

41 Lemeshko, V. V. (2002) Model of the outer membrane potential generation by the inner membrane of mitochondria. Biophys. J. **82**, 684–692.

42 Colombini, M. (1989) Voltage gating in the mitochondrial channel, VDAC. J. Membr. Biol. **111**, 103–111.

43 Colombini, M. (2012) VDAC structure, selectivity, and dynamics. Biochim. Biophys. Acta. **1818**, 1457–1465.

44 Thomas, L., Blachly-Dyson, E., Colombini, M. and Forte, M. (1993) Mapping of residues forming the voltage sensor of the voltage-dependent anion-selective channel. Proc. Natl. Acad. Sci. U.S.A. **90**, 5446–5449.

Figure Legends

Fig. 1. Formation of highly ordered, voltage-gated Type A Bax channels in a planar phospholipid membrane.

Formation of a single unit (left, N=7, 23% of all Type A experiments) under a 10 mV potential followed by three conductance drops when a 70 mV potential was applied (right). The proposed order of closure (channel ①, ③ then ②) is based on the model presented in Fig. 4.

Fig. 2. Positive cooperativity between channel ① and ②.

A single 4.4 nS conducting unit was probed using a 30 mHz (7.38 mV/sec) triangular voltage ramp (±124 mV). From top to bottom, calculated conductance, current, and voltage traces are shown, respectively. Closure of channel ② at negative potentials only occurred after closure of channel ① at a high positive potential (here at 98 mV). Note that in the absence of gating the conductance varies somewhat with voltage due to a small amount of rectification in these channels. This is typical of 5 separate experiments.

Fig. 3. Steep voltage dependence and cooperativity of channel ② and ③.

The results illustrated in Fig. 2 were supplemented with data collected later in the same experiment recorded in the presence of higher frequency rate triangular ramps (175 mHz; 43.05 mV/sec). The numbers indicate the voltages at which the channels closed or opened. Channel ② closed at nearly identical voltages (-26, -29, -27, -29 mV), whereas reopening was delayed to positive voltages due to slower kinetics. At higher frequencies (right), these slow reopening kinetics resulted in channel ② remaining closed at the positive potentials needed to close channel ③.

Fig. 4. Proposed voltage-gating model of Type A Bax channels.

Each 4.5 nS conducting unit consists of three cylindrical channels arranged in a row. Each channel is likely formed by several Bax proteins. The shading direction represents the orientation of the channels, with the middle cylinder (channel ②) having an opposite orientation compared to its neighbors. Arrows indicate the dipole moment of each channel, originating from the distribution of gating charge. The tip of the arrow is the negative end. Open circles at the end of a cylinder designate an open channel, solid circles, closed channels. Channel closure translocates the charged voltage sensor inverting the dipole moment, not the channel itself. Adjacent channels interact cooperatively, preferring to be in the same conformation: i.e. both open or both closed. This cooperativity may arise from dipole-dipole interactions between the voltage-sensor dipoles of each channel. The applied voltage is indicated by the sign at the upper right corner of each conducting unit. With no potential applied, all three channels are open (upper left). Applying a high positive voltage induces closure of channel ① whereas a negative voltage results in no closure. *Snail path*: at a constant voltage, channel closure is inhibited by the stabilizing effect of adjacent dipoles resulting in slow rates of closure. Yet a high positive voltage closes both channel ① and ③. Channel ② is forced to close through cooperativity with its neighbors, even though the sign of the voltage applied

does not favor closure. *Rabbit path*: using triangular voltage ramps, the closure of channel ① favors closure of channel ② due to the dipole-dipole interaction. Channel ② closes at negative voltages. The cooperativity between ② and ③ requires ② to be closed for ③ to close. Fast triangular voltage ramps and the slow opening kinetics of channel ② result in ② remaining closed at positive potentials, allowing channel ③ to close (all-closed mode at the lower right). From there, as the voltage is reduced either channel ③ reopens followed by channel ② or channel ③ and ② can reopen simultaneously (one-way arrow). See Fig. S4 for colored version.

Fig. 5 The voltage range at which channel ② and ③ gating occurs depends on the rate of change of transmembrane voltage

V_0 from separate experiments was plotted against the rate of change of voltage used in the experiment. The parameter was determined either in the direction that led to channel closure or in the reopening direction. A total number of 11, 10, 2, 3 experiments were used here for channel ② reopening, channel ② closure, channel ③ reopening, channel ③ closure, respectively. Typically multiple rates were tested within each experiment.

Fig. 6. Cooperative, virtually simultaneous reopening of channel ② and ③.

A single 4.5 nS conducting unit was probed with a 71 mHz (13.63 mV/sec) triangular voltage ramp. (**A**) The current recorded for 3 successive voltage ramps showing essentially simultaneous reopening of channels ② and ③. (**B**) Conductance vs. voltage plot of the data in the dotted area in (*A*). Both (*A*) and (*B*) show channel ② closure at a negative voltage, then channel ③ closing as the potential became positive, followed by simultaneous reopening of channels ② and ③. (*C*) Expanded view of the circled area in (*A*) showing that the current increased within 5 ms. This was observed in all 7, single triplet experiments.

Fig. 7 Supportive evidence of the model: multi-unit examples.

(**A**) A 2 mHz (0.28 mV/sec) triangular voltage (± 70 mV) ramp was applied to a membrane containing multiple conducting units. The voltage changed from positive to negative values and at -20 mV, 4 decrements occurred, indicating the closure of 4 channel ②'s. The remaining conductance (15 nS) is consistent with the 2 non-gating units and the 4 gating units with only channel ③'s open. Therefore at positive voltages the conductance was composed of 2 non-gating units and 4 units with their channel ① closed (3.0 nS per unit) for a total of 21 nS. (**B**) A 9 mHz (1.44 mV/sec) triangular voltage ramp (± 80 mV) was applied to the membrane resulting in conductance changes at negative potentials of 17 nS, equivalent to the closure and reopening of 11 channel ②'s (each 1.5 nS) (striped area). Thus only 11 units had a closed channel ①. The subsequent application of 70 mV for 85 s resulted in a conductance decrement of 24 nS, equivalent to the closure of 16 channel ①'s. Reapplication of the triangular voltage ramp (dotted area) showed conductance changes at negative potentials of 38 nS, equivalent to the closure and reopening of 25 channel ②'s.

Fig. 8 Estimate of the effective gating charge, n.

This is a quantitation of the gating of channel ② (see Fig. S1 and Methods for details). Points represent the n values calculated for experiments performed at the indicated rate of voltage change. The data was pooled from nine separate experiments. The solid line is the least squares fit and the dotted lines show the 95% confidence limits. The extrapolated n value at zero rate (equilibrium value) is 14 ± 2.5.

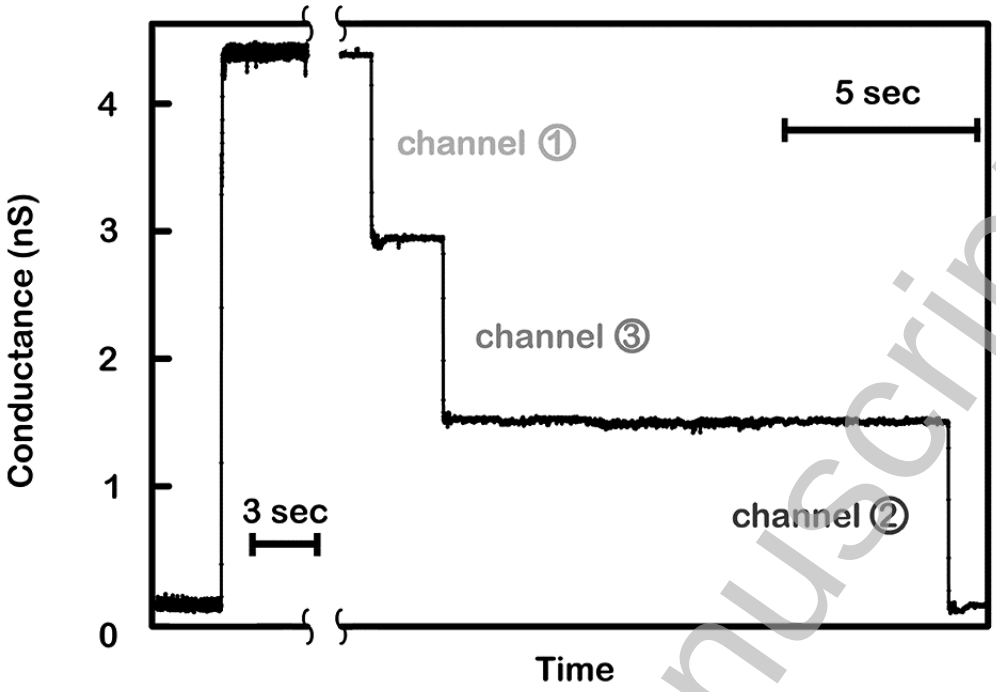

Fig. 1

Biochemical Journal Immediate Publication. Published on 06 Feb 2014 as manuscript BJ20131441

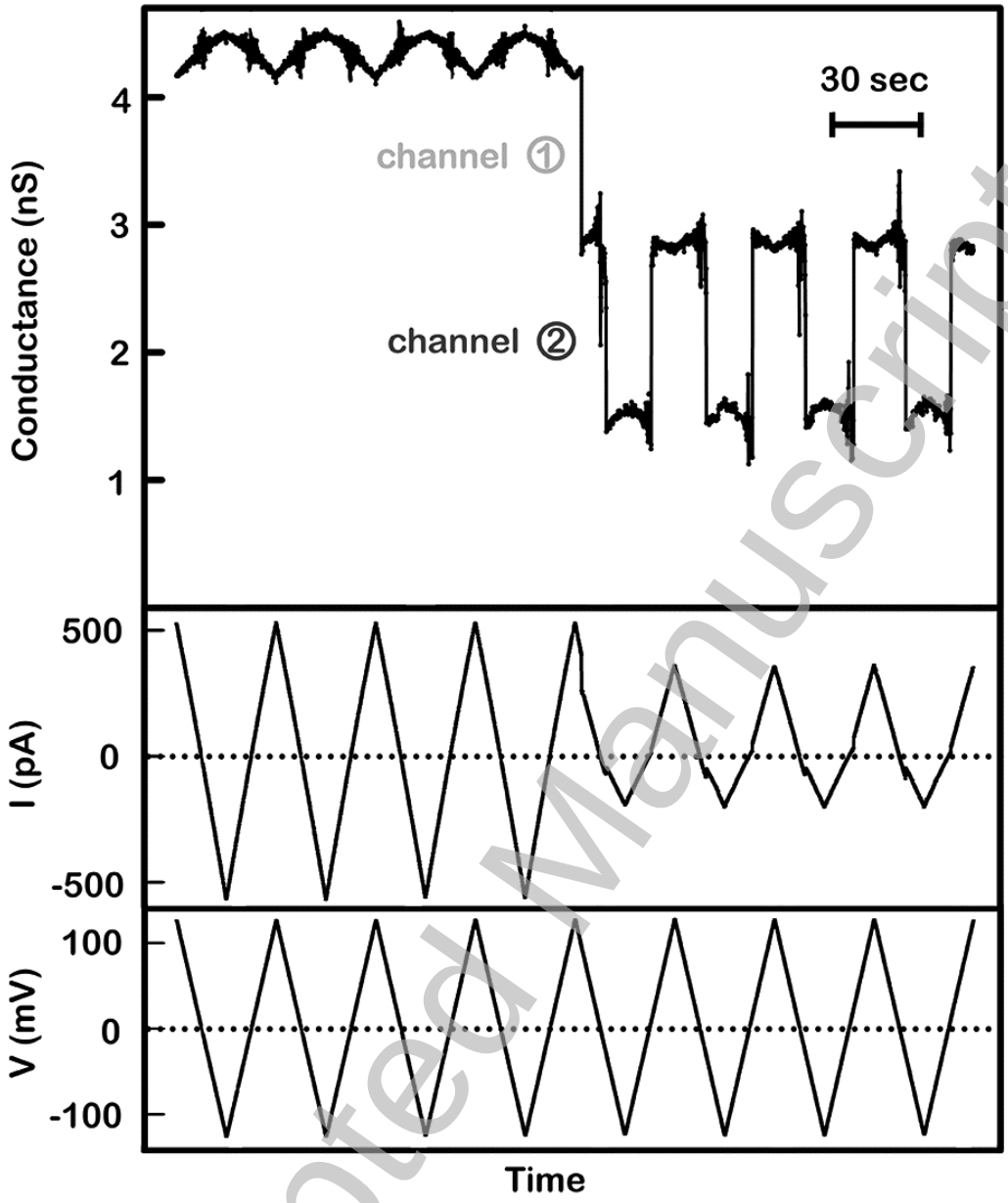

Fig. 2

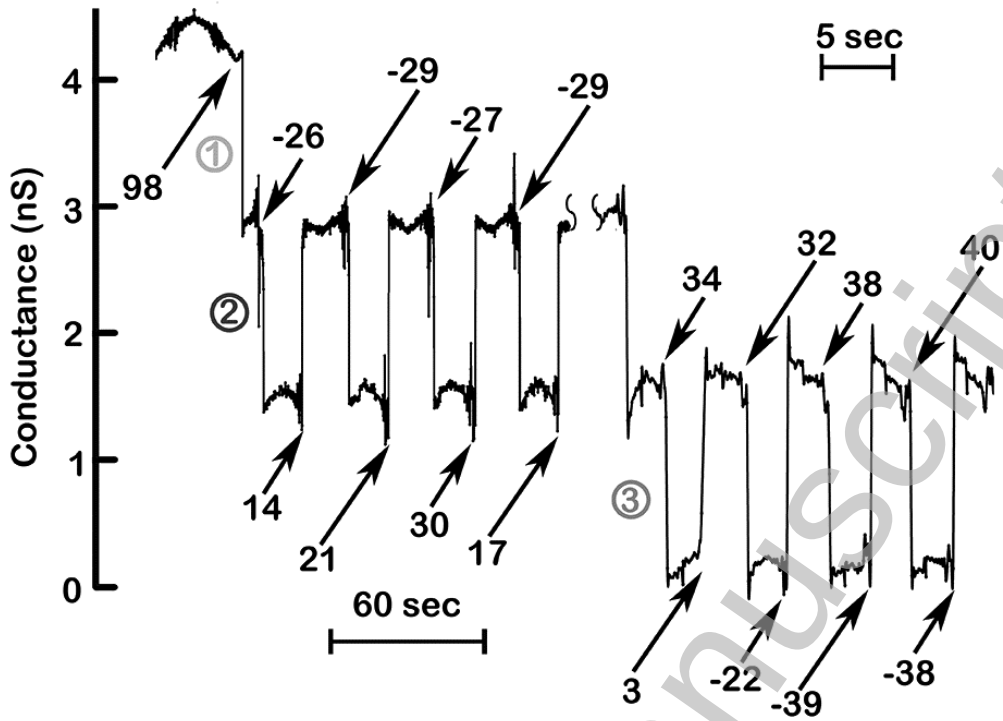

Fig. 3

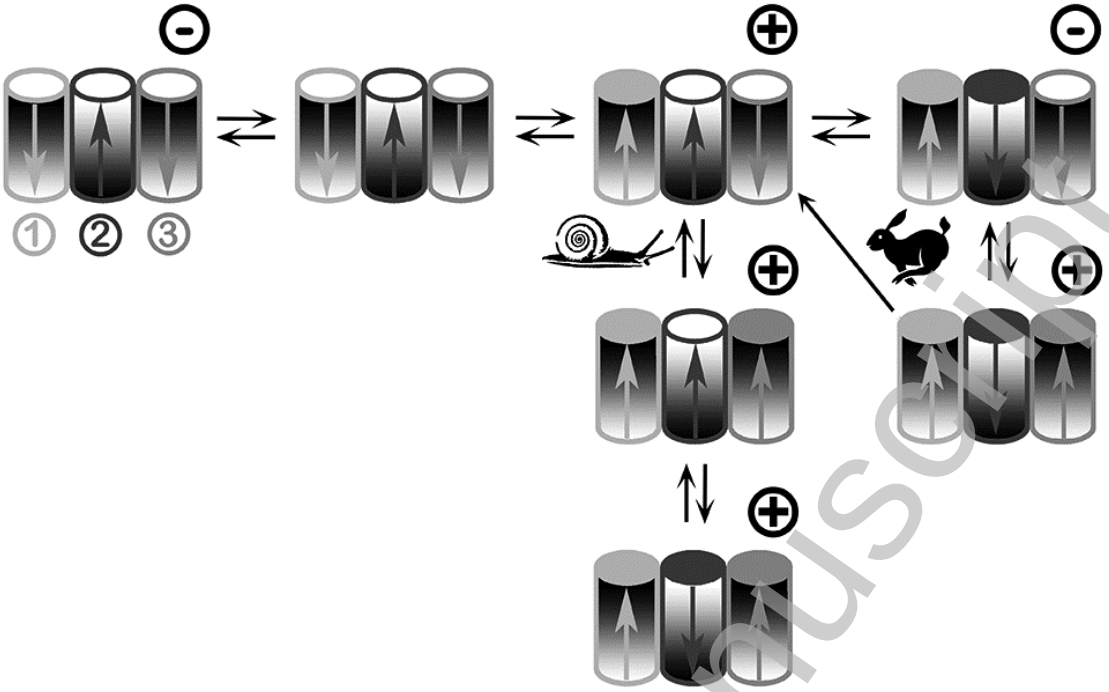

Fig. 4

Biochemical Journal Immediate Publication. Published on 06 Feb 2014 as manuscript BJ20131441

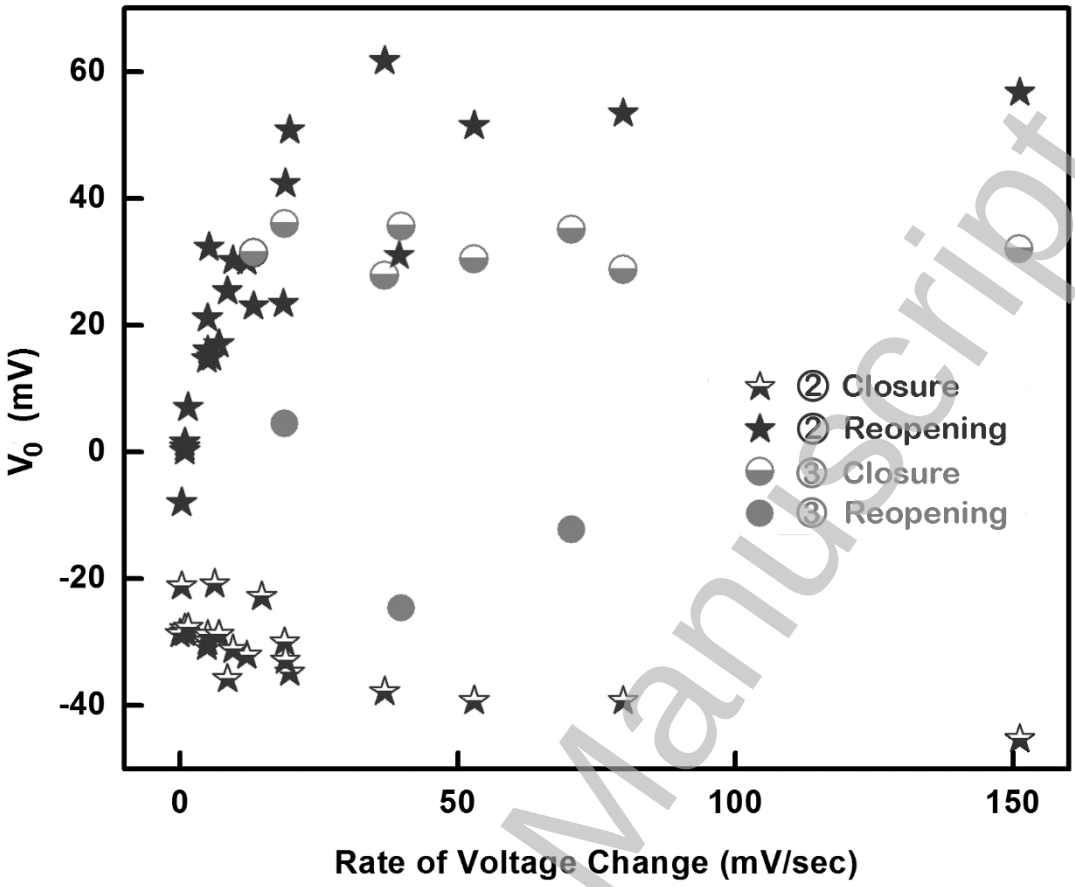

Fig. 5

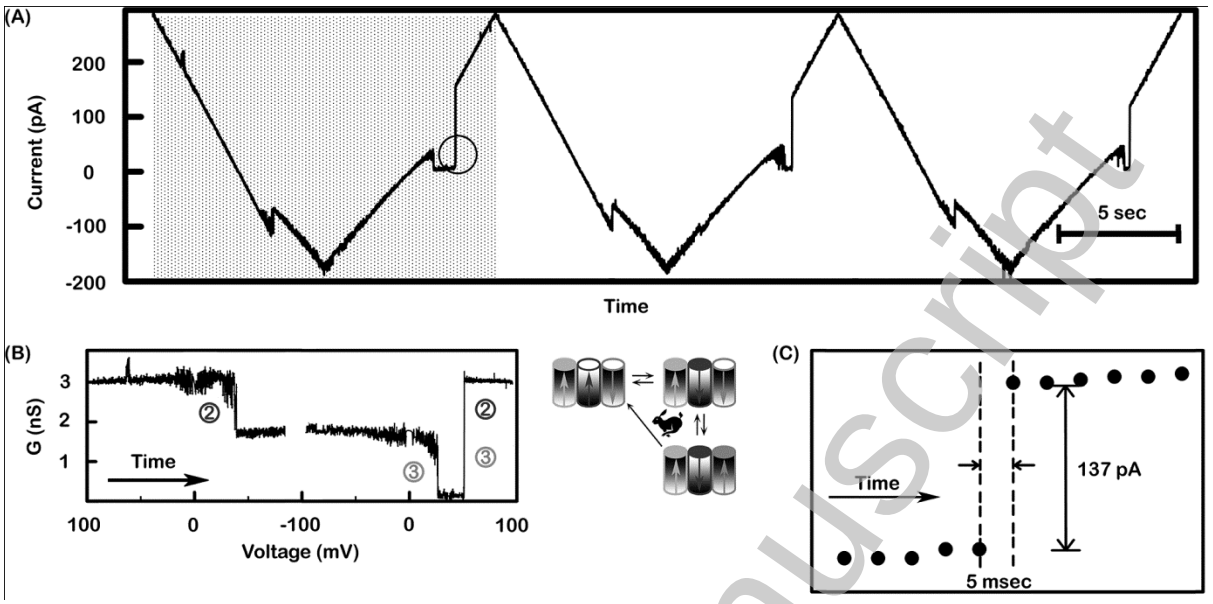

Fig. 6

Biochemical Journal Immediate Publication. Published on 06 Feb 2014 as manuscript BJ20131441

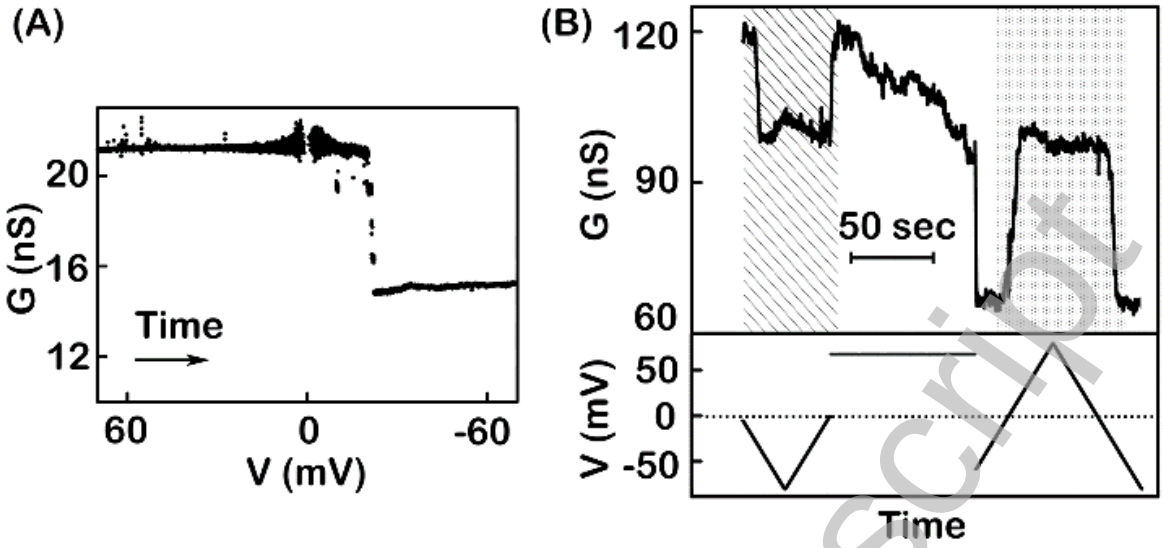

Fig. 7

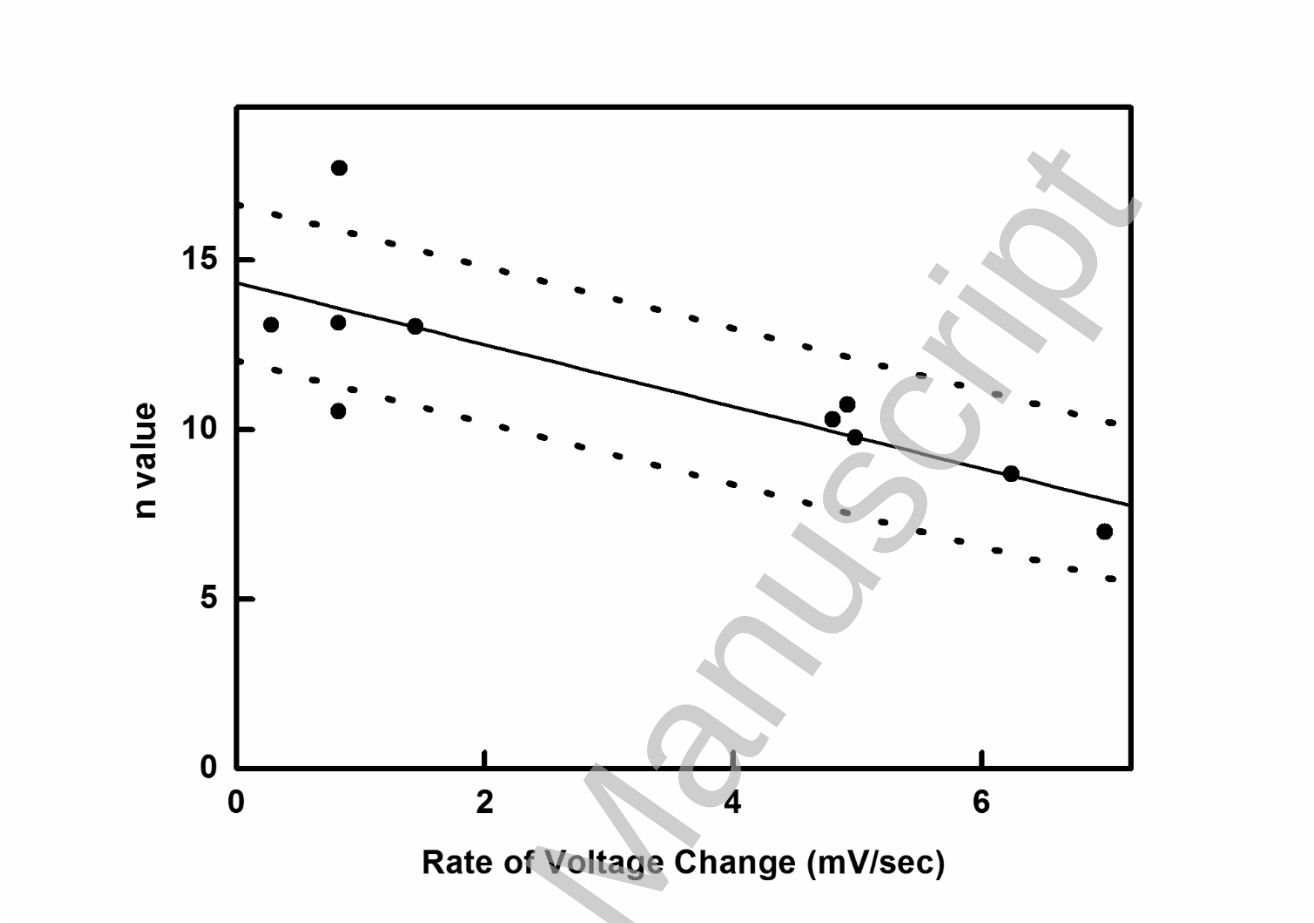

Fig. 8